

Supplemental information

**The structural basis of *Salmonella* A₂B₅
toxin neutralization by antibodies targeting
the glycan-receptor binding subunits**

Tri Nguyen, Angelene F. Richards, Durga P. Neupane, J. Ryan Feathers, Yi-An Yang, Ji Hyun Sim, Haewon Byun, Sohyoung Lee, Changhwan Ahn, Greta Van Slyke, J. Christopher Fromme, Nicholas J. Mantis, and Jeongmin Song

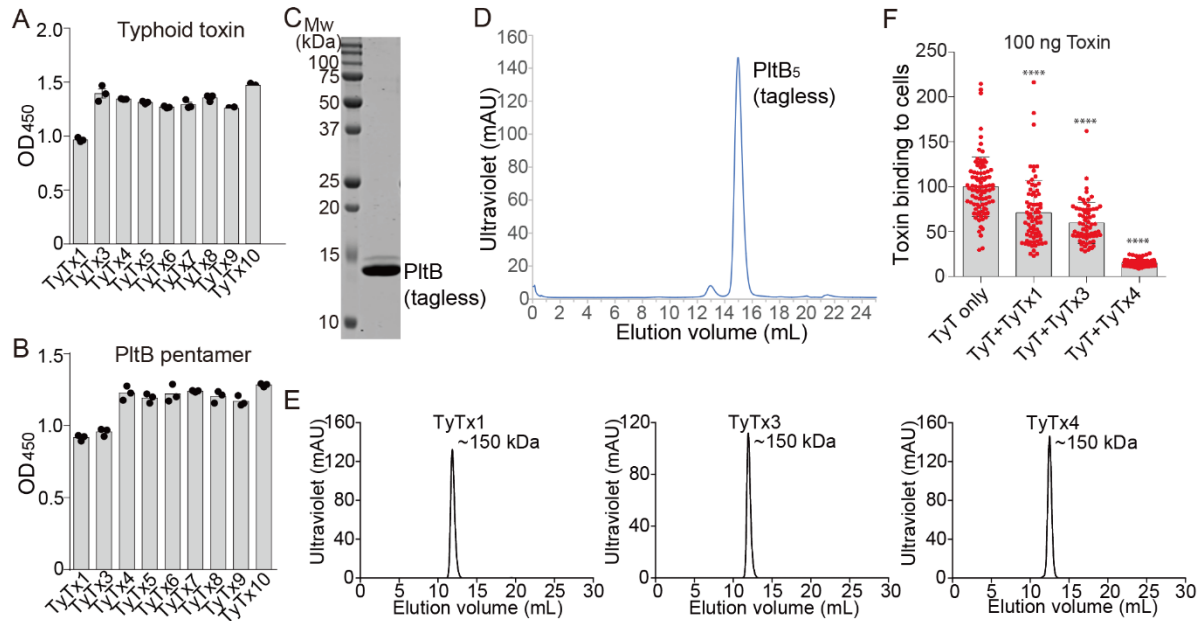


Figure S1. MAb ELISAs, Size-exclusion chromatograms, MAb-mediated inhibition of typhoid toxin binding to Henle-407 cells, and purified recombinant tagless PltB, related to Fig. 1A-C and 4. A-B, MAb ELISAs were performed to determine their specificities towards typhoid toxin (**A**) and tagless PltB pentamer (**B**). Bars represent the mean values of three replicates, which were obtained by measuring the absorbance at 450 nm. **C-D**, SDS-PAGE (**C**) and size-exclusion chromatograms (**D**) of purified recombinant PltB (tagless). See also the experimental procedure section for details. **E**, SD200 chromatograms of TyTx1 (left panel), TyTx3 (middle), and TyTx4 (right). Superdex 200 Increase prepacked columns (Cytiva) was used. **F**. Henle-407 cells grown on coverslips were precooled to 4°C, incubated with 100 ng of typhoid toxin-AF555 in the presence or absence of 2 µg MAb for 30 min, counterstained with DAPI, and analyzed by fluorescent microscopy. Bars represent the mean ± SEM obtained from at least three independent experiments. Each dot reflects the typhoid toxin signal intensity per image. n=60-88. ****, p<0.0001, compared to the TyT only group. Two-tailed unpaired t-tests were performed.

```

TyTx7LCVariable      -MGP HKLR ES LKMVSTPQFLVFLFWIPASRGDILLTQSPSILSVSPGERVVFSCRASQS
TyTx8LCVariable      -----MVSTPQFLVFLFWIPASRGDILLTQSPSILSVSPGERVVFSCRASQS
TyTx10LCVariable     -----MVSTPQFLVFLFWIPASRGDILLTQSPSILSVSPGERVVFSCRASQS
TyTx6LCVariable      -----MVSTPQFLVFLFWIPASRGDILLTQSPSILSVSPGERVVFSCRASQS
TyTx9LCVariable      MGGPHKLR ES LKMVSTPQFLVFLFWIPASRGDILLTQSPSILSVSPGERVVFSCRASQS
TyTx5LCVariable      MGGPHKLR ES LKMVSTPQFLVFLFWIPASRGDILLTQSPSILSVSPGERVVFSCRASQS
TyTx4LCVariable     MGGPHKLR ES LKMVSTPQFLVFLFWIPASRGDILLTQSPSILSVSPGERASFSCRASQS
TyTx3LCVariable      -----MRPSIQFLGLLFWLHGAQC DIQMTQSPSSLASLGGKVTITCKASQD
TyTx1LCVariable     -----MDSQAQVLIILLLLWVSGTCCD IVMQSPSSLAVSAGEKVTMSCKSSQS
                        *      *. * : ** : .      ** : : ** . * * : . * * : : * : : * :
TyTx7LCVariable      IG-----TSIHWYQQKPNQSPRLLIQYASQSI SGIPSRFSGSGSGTDFTLTINSVESED
TyTx8LCVariable      IG-----TSIHWYQQKPNQSPRLLIQYASQSI SGIPSRFSGSGSGTDFTLTINSVESED
TyTx10LCVariable     IG-----TSIHWYQQKPNQSPRLLIQYASQSI SGIPSRFSGSGSGTDFTLTINSVESED
TyTx6LCVariable      IG-----TSIHWYQQKPNQSPRLLIQYASQSI SGIPSRFSGSGSGTDFTLTINSVESED
TyTx9LCVariable      IG-----TSIHWYQQKPNQSPRLLIQYASQSI SGIPSRFSGSGSGTDFTLTINSVESED
TyTx5LCVariable      IG-----TSIHWYQQKPNQSPRLLIQYASQSI SGIPSRFSGSGSGTDFTLTINSVESED
TyTx4LCVariable     IG-----TSIHWYQQKPNQSPRLLIQYASQSI SGIPSRFSGSGSGTDFTLTINSVESED
TyTx3LCVariable      IN-----KYIAWYQHKPKGKPRLLIHYTSTLQPDIPSRFSGSGSGRDYSFISINLEPED
TyTx1LCVariable     LFNSRTRKNHLAWYQQKPGQSPKLLIYWASTGESGVPDRFTGSGSGTDFTLTISSVQAED
                        :      . : * : * : * : * : * : * : * : * : * : * : * : * : * : * : * : * :
TyTx7LCVariable      IADYYCQHTNGWPYTFGGGT TLEINRADAAPT VSI FPPSSEQLTSGGASVVCFLNNFYPK
TyTx8LCVariable      IADYYCQHTNGWPYTFGGGT TLEINRADAAPT VSI FPPSSEQLTSGGASVVCFLNNFYPK
TyTx10LCVariable     IADYYCQHN-GWPYTFGGGT TLEINRADAAPT VSI FPPSSEQLTSGGASVVCFLNNFYPK
TyTx6LCVariable      IADYYCQHTNGWPYTFGGGT TLEINRADAAPT VSI FPPSSEQLTSGGASVVCFLNNFYPK
TyTx9LCVariable      IADYYCQHTNGWPYTFGGGT TLEINRADAAPT VSI FPPSSEQLTSGGASVVCFLNNFYPK
TyTx5LCVariable      IADYYCQHTNGWPYTFGGGT TLEINRADAAPT VSI FPPSSEQLTSGGASVVCFLNNFYPK
TyTx4LCVariable     IADYYCQHTNGWPYTFGGGT TLEINRADAAPT VSI FPPSSEQLTSGGASVVCFLNNFYPK
TyTx3LCVariable      IATYYCLOYDTFLRTFGGGTKLEIKRADAAPT VSI FPPSSEQLTSGGASVVCFLNNFYPK
TyTx1LCVariable     LAVYFCQSYNRA LTFGSGTKLELKRADAAPT VSI FPPSSEQLTSGGASVVCFLNNFYPK
                        : * * : * :      * : * : * : * : * : * : * : * : * : * : * : * : * : * : * : * :
TyTx7LCVariable      DINVMVYLLLLKVKQNYSRGN-
TyTx8LCVariable      DINVMVYLLLLKVKQNYSEGIS
TyTx10LCVariable     DINVMVYLLLLKVKQNIREF--
TyTx6LCVariable      DINVMVYLLLLKVNKIFRGN--
TyTx9LCVariable      DINVMVYLLLLKVNKIFQRGIS
TyTx5LCVariable      DINVMVYLLLLKVKQNI RGS--
TyTx4LCVariable     DINVMVYLLLLKVNKIFRGEFR
TyTx3LCVariable      DINVMVYLLLLKVKQNIQREFL
TyTx1LCVariable     DINVMVYLLLLKVKQNYSGNS-
                        ***** : :

```

Figure S2. Amino acid sequences of the light (kappa) chain variable region of TyTx1-10, related to Figs. 1-3. Highlighted in bold are the MAbs whose epitopes have been defined via cryo-EM in this study. The first amino acid residues indicated in the cryo-EM structures deposited are highlighted in red. Amino acid residues that bind to the toxin are highlighted in cyan.

TyTx5HeavyVariable	MNFGPSLI FLVLILKGVQCEVKLVESGGGLVKPGGSLKLSCAASGFAFSTYDMSWVRQTP
TyTx10HeavyVariable	MNFGPSLI FLVLILKGVQCEVKLVESGGGLVKPGGSLKLSCAASGFAFSTYDMSWVRQTP
TyTx9HeavyVariable	MNFGPSLI FLVLILKGVQCEVKLVESGGGLVKPGGSLKLSCAASGFAFSTYDMSWVRQTP
TyTx6HeavyVariable	MNFGPSLI FLVLILKGVQCEVKLVESGGGLVKPGGSLKLSCAASGFAFSTYDMSWVRQTP
TyTx8HeavyVariable	MNFGPSLI FLVLILKGVQCEVKLVESGGGLVKPGGSLKLSCAASGFAFSTYDMSWVRQTP
TyTx7HeavyVariable	MNFGPSLI FLVLILKGVQCEVKLVESGGGLVKPGGSLKLSCAASGFAFSTYDMSWVRQTP
TyTx4HeavyVariable	MNFGPSLI FLVLILKGVQCEV K LVESGGGLVKPGGSLKLSCAASGFAFSTY D MSWVRQTP
TyTx1HeavyVariable	--MERRWFI FLV L GNAGMH C E I QSQQCGPELVKPGSSVKVSKASGYAFTNYKALGSKQSH
TyTx3HeavyVariable	MGWSCIIFFLVATATGVHSVQLQSQSGPEVVRPGVSVKISCKGSGYTFFTDYAMHWVKQSH : : : : * : . : : : . : * : * : * * * : * : * : * : * : * : * :
TyTx5HeavyVariable	EKRLEWVATISGGGSYTYYPDIVKGRFTISRDNARNTLYLQMSLRSSEDTALYFCVRQYY
TyTx10HeavyVariable	EKRLEWVATISGGGSYTYYPDIVKGRFTISRDNARNTLYLQMSLRSSEDTALYFCVRQYY
TyTx9HeavyVariable	EKRLEWVATISGGGSYTYYPDIVKGRFTISRDNARNTLYLQMSLRSSEDTALYFCVRQYY
TyTx6HeavyVariable	EKRLEWVATISGGGSYTYYPDIVKGRFTISRDNARNTLYLQMSLRSSEDTALYFCVRQYY
TyTx8HeavyVariable	EKRLEWVATISGGGSYTYYPDIVKGRFTISRDNARNTLYLQMSLRSSEDTALYFCVRQYY
TyTx7HeavyVariable	EKRLEWVATISGGGSYTYYPDIVKGRFTISRDNARNTLYLQMSLRSSEDTALYFCVRQYY
TyTx4HeavyVariable	EKRLEWVATISGGGSYTYYPDIVKGRFTISRDNARNTLYLQMSLRSSEDTALYFCVRQYY
TyTx1HeavyVariable	GKSLEWIGY I DP Y NS D S Y NP Q FKDKATLTVDKSSSTAYMYLNSLTSSEDSAVYYCAG--L
TyTx3HeavyVariable	AKSLEWIGIVISTYTGNTKYNQNFKGKATMTVDKSSSTAYMELARLTSSEDSAIYYCARNYR * * * * . : * . . : * : . * . : * : * : * : * : * : * : * * * * . : * * * * . : * * * * .
TyTx5HeavyVariable	GSSNYGMDYWQGQTSVTVSSAKTTAPSVYPLAPVCGDTTGSSVTLGCLVKGYFPEPVTLT
TyTx10HeavyVariable	GSSNYGMDYWQGQTSVTVSSAKTTAPSVYPLAPVCGDTTGSSVTLGCLVKGYFPEPVTLT
TyTx9HeavyVariable	GSSNYGMDYWQGQTSVTVSSAKTTAPSVYPLAPVCGDTTGSSVTLGCLVKGYFPEPVTLT
TyTx6HeavyVariable	GSSNYGMDYWQGQTSVTVSSAKTTAPSVYPLAPVCGDTTGSSVTLGCLVKGYFPEPVTLT
TyTx8HeavyVariable	GSSNYGMDYWQGQTSVTVSSAKTTAPSV-----
TyTx7HeavyVariable	GSSNYGMDYWQGQTSVTVSSAKTTAPSVYPLAPVCGDTTGSSVTLGCLVKGYFPEPVTLT
TyTx4HeavyVariable	GSS N YGMDYWQGQTSVTVSSAKTTAPSVYPLAPVCGDTTGSSVTLGCLVKGYFPEPVTLT
TyTx1HeavyVariable	ELTG-TLPYWQGQTLVTVSSAKTTAPSVYPTGPWICPN-----
TyTx3HeavyVariable	YDGEYYFDYWQGQTTTLTVSSAKTTAPSVYPLAPGSAAQTNMVTLGCLVKGYFPEPVTVI : * * * * * : * * * * * . * * * *
TyTx5HeavyVariable	S--GSPWYISFLK-----
TyTx10HeavyVariable	S--GSPWYISFLKLNKIFEF--
TyTx9HeavyVariable	S--GSPWYISFLK-----
TyTx6HeavyVariable	W--IPMVYLLKVNKIFRGNF-
TyTx8HeavyVariable	-----
TyTx7HeavyVariable	-----
TyTx4HeavyVariable	WNSGSPWYISFLK-----
TyTx1HeavyVariable	-----
TyTx3HeavyVariable	LDPHGISPS-----

Figure S3. Amino acid sequences of the heavy chain variable region of TyTx1-10, related to Figs. 1-3. Highlighted in bold are the antibodies whose epitopes have been defined via cryo-EM in this study. The first amino acid residues indicated in the cryo-EM structures deposited are highlighted in red. Amino acid residues that bind to the toxin are highlighted in purple.

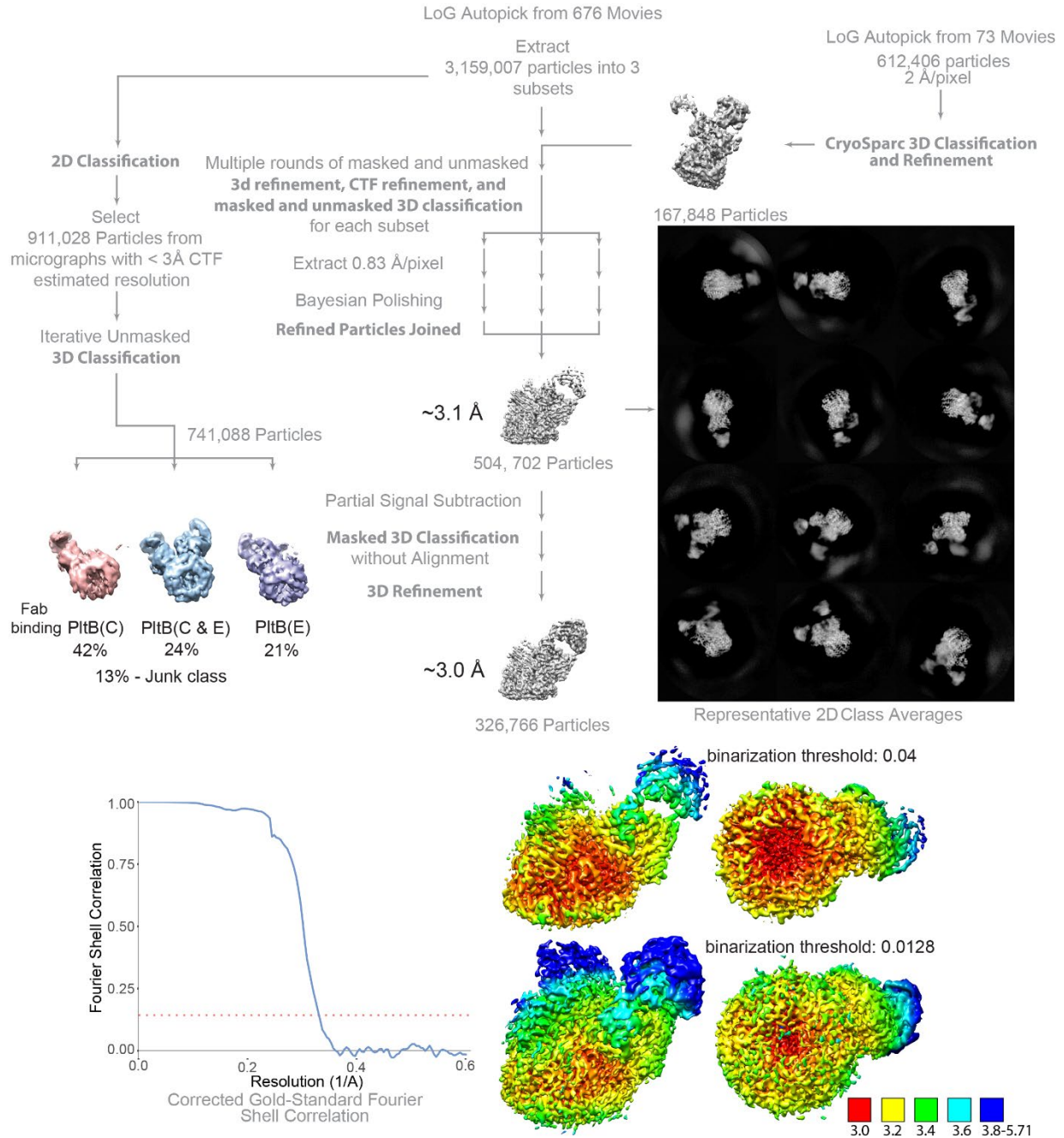


Figure S4. Flow chart depicting the cryo-EM workflow of the TyTx1 Fab-toxin complexes, related to Fig. 2. Details are described in the experimental procedure section under cryo-EM, data collection, and structure determination. Color-coded local resolution map is shown on the bottom right. The resolution map generated using 'binarization threshold=0.04' (top panel) is shown in the flow chart, while the map generated using 'binarization threshold=0.0128' is shown in the bottom panel that matches with Fig. 2B. Note that the FSC curve remains the same because the FSC curve was generated as part of post-processing of cryo-EM image refinement before any visualization steps for preparing figure panels. The appearance of the resolution maps can be different depending on the 'binarization threshold' value used during visualization. The local resolution maps were generated by Relion and visualized by Chimera.

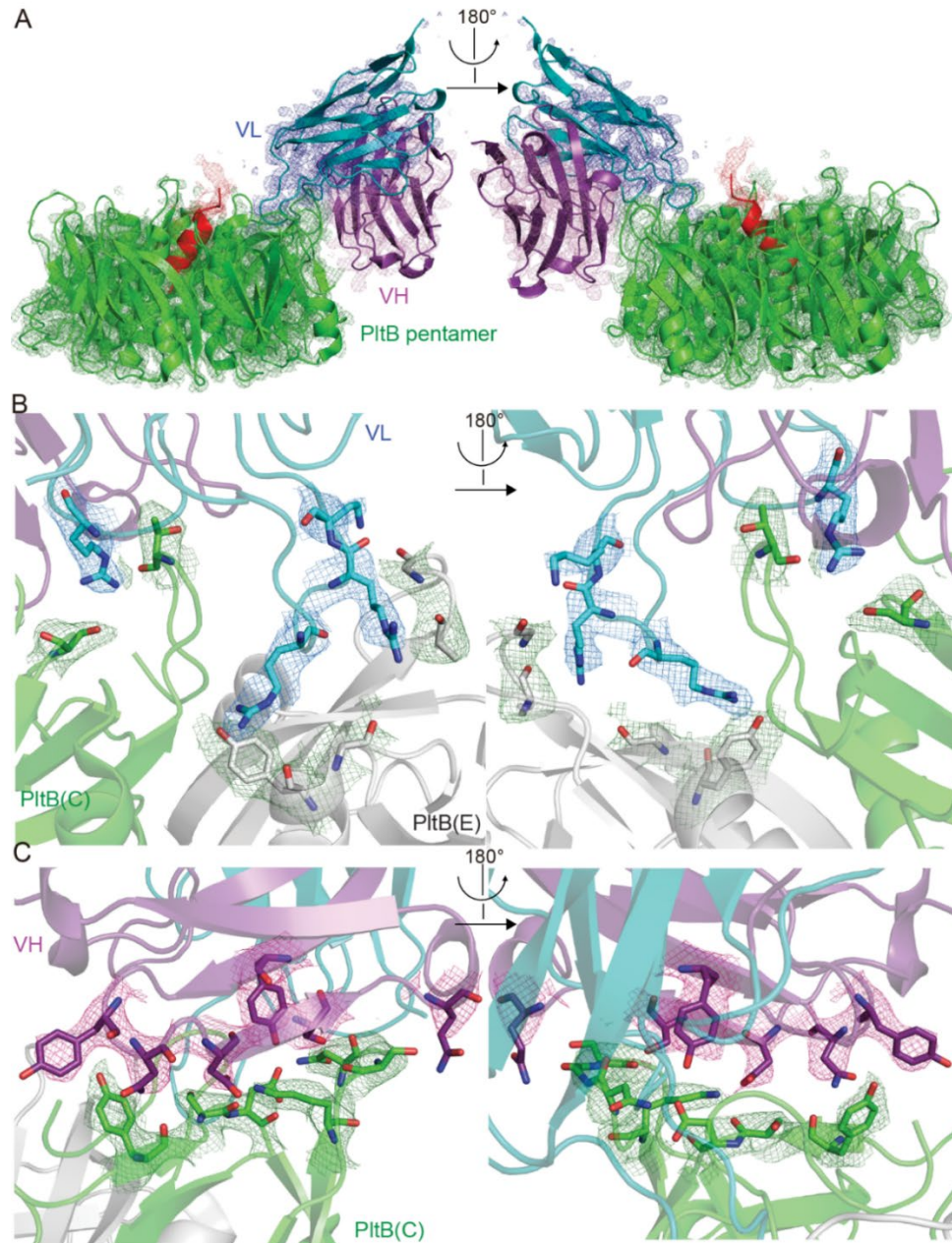


Figure S5. Cryo-EM density maps of typhoid toxin PltB pentamer bound to TyTx1 Fab variable regions, related to Fig. 2B-E. **A**, Overall cryo-EM density maps of PltB pentamer bound to TyTx1 variable regions of the light chain (VL, blue) and the heavy chain (VH, purple). The red helix is the tail part/C-terminal α -helix of PltA. **B-C**, Density maps of the interface between PltB subunits (C chain, green and E chain, grey) and TyTx1 VL (blue) (**B**) and between PltB subunits and TyTx1 VH (purple) (**C**). The density mesh was generated through Pymol based on the CryoEM density map around the built molecular structure. Color-coded local resolution map is shown in Fig S4, explaining the missing density in some parts.

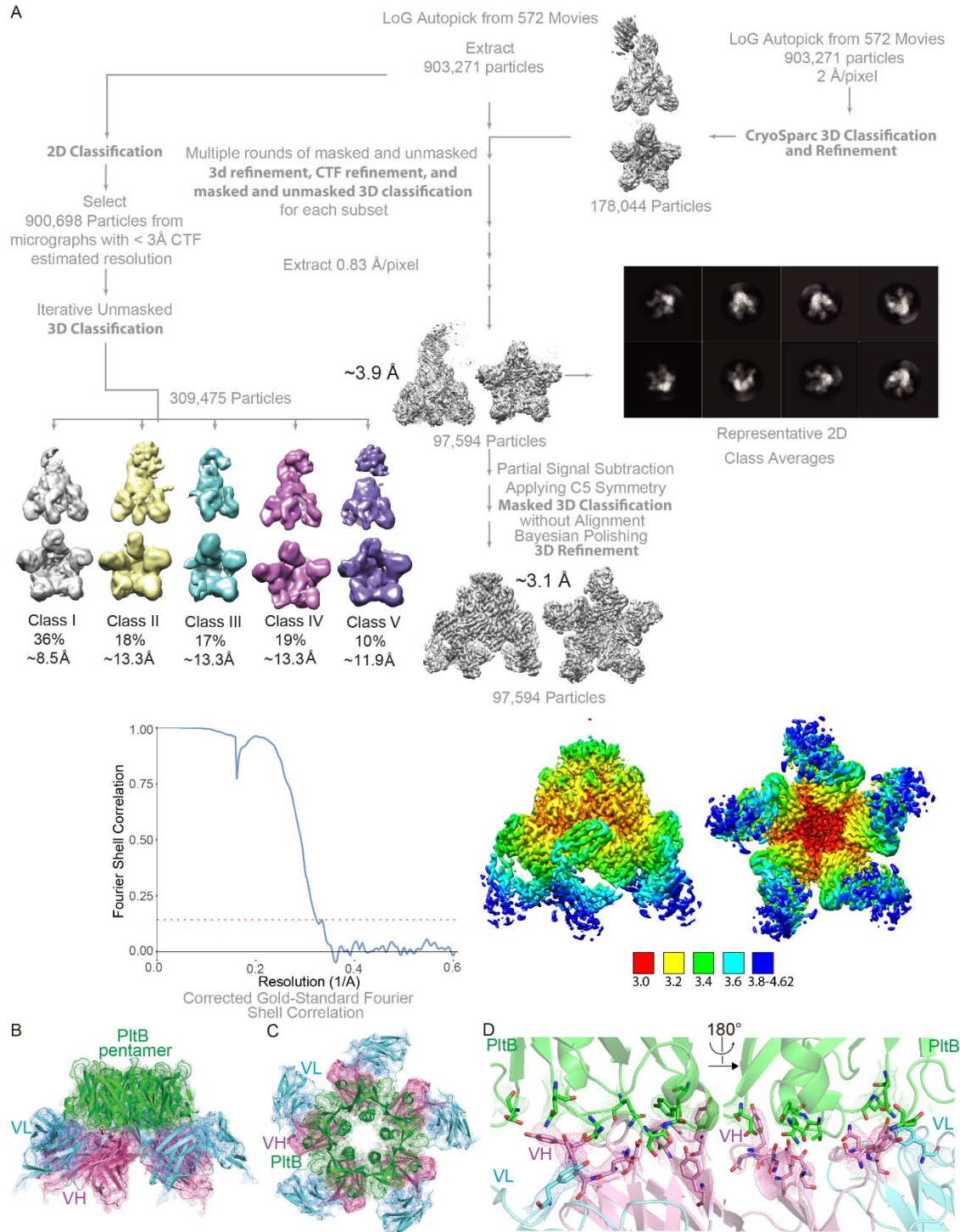


Figure S6. Cryo-EM workflow of the TyTx4 Fab-toxin complexes and cryo-EM density maps, related to Fig. 3A-D. **A**, Cryo-EM workflow. Details are described in the experimental procedure section under cryo-EM, data collection, and structure determination. Color-coded local resolution map is shown on the bottom right. **B-C**, Side (**B**) and top views (**C**) of overall cryo-EM density maps of PitB pentamer bound to TyTx4 variable regions of the light chain (VL, light blue) and the heavy chain (VH, pink). **D**, Density maps of the interface between PitB pentamer (green) and TyTx4 VL (light blue) and VH (pink). The density mesh was generated through Pymol based on the CryoEM density map around the built molecular structure.

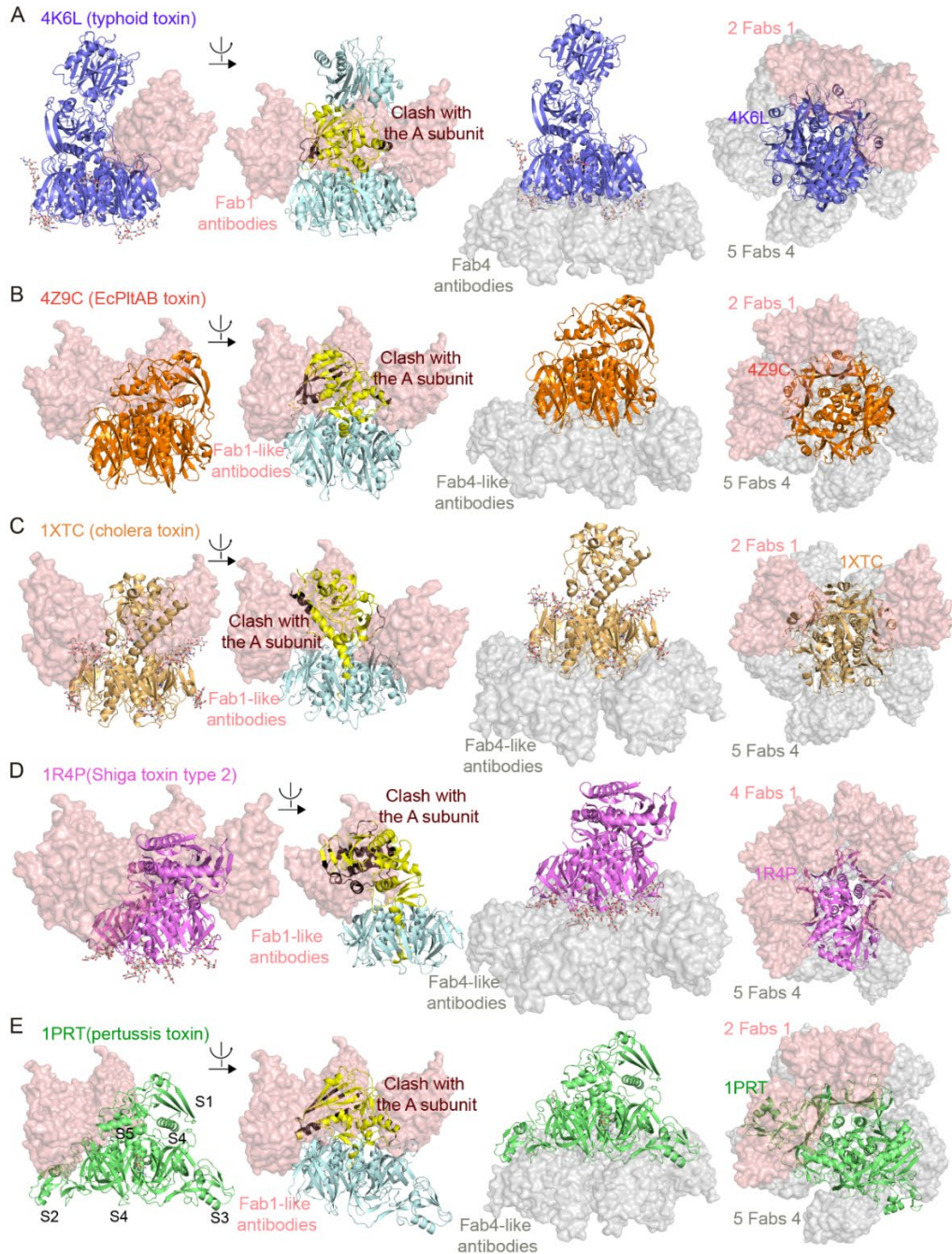


Figure S7. Secondary structure matching (SSM) analyses of bacterial AB₅ toxins, related to Fig. 7. A-E, Typhoid toxin (A), *E. coli* PltAB toxin (B), cholera toxin (C), Shiga toxin type 2 (D), and pertussis toxin (E) are complexed with TyTx1 Fabs (pink volume) and TyTx4 Fabs (grey volume). The region of toxin encroaching the TyTx1 Fab volume was manually identified and highlighted in brown (clashes with the A subunit in yellow). Total numbers of Fabs that can bind to the indicated toxins without clashes are indicated in the top view images that overlay toxin, Fabs of TyTx1, and Fabs of TyTx4 (the far right panel). Glycan receptor moieties are also indicated if known; See also Table S5. Note that unlike all other A₂B₅ toxins investigated in this manuscript (where up to 2 Fabs 1 or up to 5 Fabs 4 can fit in), our SSM analyses predict that 4 Fabs 1 or 5 Fabs 4 can fit in the region around the B subunit of Shiga toxin without clashes. We hypothesize that the A-subunit mediated asymmetry combined with a relatively smaller Shiga toxin contributes to this prediction result. This theoretical prediction appears to be highly conservative based on a recent observation by Bernedo-Navarro and colleagues (Bernedo-Navarro et al., 2018).

Table S1. Cryo-EM data collection, refinement, and validation statistics, related to Figs. 2-3.

	TyTx1-Toxin Complex (EMDB-22699) (PDB 7K7H)	TyTx4-Toxin Complex (EMDB-22700) (PDB 7K7I)
Data collection and processing		
Magnification	49,000	49,000
Voltage (kV)	200	200
Electron exposure (e-/Å ²)	53.0	51.5
Defocus range (µm)	-0.8 to -1.5	-0.8 to -1.5
Pixel size (Å)	1.66	1.66
Symmetry imposed	C1	C5
Initial particle images (no.)	3,159,007	903,271
Final particle images (no.)	326,766	97,594
Map resolution (Å)	3.00	3.13
FSC threshold	0.143	0.143
Map resolution range (Å)	2.6 to 3.4	3.0 to 3.7
Refinement		
Initial models used (PDB code)	4RHR, 1MHH, 4H20	4RHR, 2OZ4, 4M48,
Model resolution (Å)	3.00	3.13
FSC threshold	0.143	0.143
Model resolution range (Å)	2.63 to 3.38	2.97 to 3.69
Map sharpening <i>B</i> factor (Å ²)	83.57	101.11
Model composition		
Non-hydrogen atoms	6320	13195
Protein residues	816	1705
Ligands	0	0
<i>B</i> factors (Å ²)		
Protein	36.89	55.14
Ligand	0	0
R.m.s. deviations		
Bond lengths (Å)	0.003	0.003
Bond angles (°)	0.517	0.530
Validation		
MolProbity score	1.95	2.17
Clashscore	8.45	11.29
Poor rotamers (%)	0	0
Ramachandran plot		
Favored (%)	91.88	87.82
Allowed (%)	8.12	12.18
Disallowed (%)	0	0

Table S2. PltB amino acid residues known to interact with glycan-receptors, related to Figs. 2-3.
 Note that binding pocket BS1 is located on the lateral side of PltB pentamer, whereas binding pockets BS2 and BS3 are located on the bottom side of PltB pentamer.

Glycan receptors*	Methods used	Residues in BS1**	Residues in BS2**	Residues in BS3**	References
Neu5Ac	Molecular docking	Y33, S35 , K59			(Song et al., 2013)
Neu5Ac α 2-6Gal β 1-4GlcNAc	Co-crystal structure	Y33, Y34, S35, K59, R100			(Lee et al., 2020)
Neu5,9Ac α 2-6Gal β 1-4GlcNAc	Co-crystal structure	Y34, S35, K59, T65, R100			(Nguyen et al., 2020)
Neu5Ac α 2-3Gal β 1-4GlcNAc	Co-crystal structure	Y33, Y34, S35 , D36, K59 , R100	Q75, I107, W108 , T109 , Y110, F113	E24, D28 , N29 , D48, Y110	(Lee et al., 2020)
Neu5,9Ac α 2-3Gal β 1-4GlcNAc	Co-crystal structure	Y33, Y34, S35, K59, N61, T65, R100	Q75, I107, W108, T109, Y110, F113		(Nguyen et al., 2020)
Neu4,5Ac α 2-3Gal β 1-4GlcNAc	Co-crystal structure	Y33, Y34, S35, D36, K59, T65	Q75, W108, T109, Y110		(Nguyen et al., 2020)
GD2 glycan: GalNAc β 1-4(Neu5Ac α 2-8Neu5Ac α 2-3)Gal β 1-4Glc	Co-crystal structure	Y33 , Y34, S35 , K59 , T65, R100			(Deng et al., 2014)

* Neu5Ac, N-acetylneuraminic acid; Gal, galactose; GlcNAc, N-acetylglucosamine; Neu5,9Ac α 2, 9-O-acetyl Neu5Ac; Neu4,5Ac α 2, 4-O-acetyl Neu5Ac; GalNAc, N-acetylgalactosamine; Glc, glucose.

** Residues in bold, their importance was experimentally confirmed through mutagenesis studies in references indicated.

Table S3. Primers used in this study, related to Fig. 1 and STAR Methods.

Application	Primer name	Forward or reverse	Primer sequence (5'-3')
Reverse transcription	Template-switch oligo	Universal forward primer	AGGCAGTGGTATCAACGCAGAGTACATGrGrGr
	mIGK RT	Reverse primer for kappa chain	TTGTCGTTCACTGCCATCAATC
	mIGL RT	Reverse primer for lambda chain	GGGTACCATCTACCTTCCAG
	mIGHG RT	Reverse primer for heavy chain	AGCTGGGAAGGTGTGCACAC
PCR	ISPCR	Universal forward primer	AAGCAGTGGTATCAACGCAGAG
	mIGK PCR	Reverse primer for kappa chain	ACATTGATGTCTTTGGGGTAGAAG
	mIGL PCR	Reverse primer for lambda chain	ATCGTACACACCAGTGTGGC
	mIGHG PCR	Reverse primer for heavy chain	GGGATCCAGAGTTCCAGGTC

GrGrGr: 3 riboguanines. See Meyer et al, 2019 for details (Meyer et al., 2019).

Table S4. Kinetics of TyTx MAbs binding to typhoid toxin by surface plasmon resonance (SPR) assays, related to Fig. 5.

MAb	Isotype	Target	k_a ($M^{-1}s^{-1}$)^a	k_d (s^{-1})^a	K_D (M)^a
TyTx1	IgG1	PltB	9.39×10^4	6.64×10^{-3}	7.11×10^{-8}
TyTx3	IgG1	PltB	1.73×10^5	1.68×10^{-2}	1.45×10^{-7}
TyTx4	IgG2a	PltB	1.03×10^6	6.80×10^{-6}	6.70×10^{-12}

^a Mean values of three technical replicates.

Table S5. Secondary structure matching analyses of bacterial AB₅ toxins, related to Fig. 7.

Toxin name	Holotoxin PDB	Glycan complex PDB (glycan name) ¹	TyTx1-like IgGs per toxin (shoulder-located epitopes).	TyTx4-like IgGs per toxin (bottom-located epitopes)
Typhoid toxin (A ₂ B ₅)	4K6L	6P4M (Neu5Acα2-3Galβ1-4GlcNAc)	1 MAb (2 Fabs)	3 MAbs (5 Fabs)
<i>E. coli</i> PltAB toxin (AB ₅)	4Z9C	Unknown ²	1 MAb (2 Fabs)	3 MAbs (5 Fabs)
Cholera toxin (AB ₅) ³	1XTC	5ELB (Lewis Y glycans); 2CHB (GM1 glycans)	1 MAb (2 Fabs)	3 MAbs (5 Fabs)
Shiga toxin type 2 (AB ₅) ⁴	1R4P	1BOS (α-D-galactopyranose-(1-4)-β-D-galactopyranose-(1-4)-β-D-glucopyranose).	2 MAbs (4 Fabs)	3 MAbs (5 Fabs)
Pertussis toxin (AB ₅) ⁵	1PRT	1PTO (Neu5Acα2-6-β-D-galactopyranose)	1 MAb (2 Fabs)	3 MAbs (5 Fabs)

¹Additional glycan binding pockets may exist.

²Glycan bound structure is unavailable.

³Similar to typhoid toxin, glycan-binding pockets are located on both the shoulder and the bottom.

⁴Glycan binding pockets are located on the bottom side of the B pentamer.

⁵Glycan binding pockets on the shoulder regions in S2 and S3. Heteropentameric B subunits consisting of S2, S3, 2S4, and S5 can also be considered as an intrinsic immune subversion mechanism because their epitopes in the B heteropentamer are different.

Table S6. Comparison of *S. Typhi* *pltB* sequences deposited in NCBI, related to Fig. 6. Shown are the first 100 hits from the BLAST search using *S. Typhi* CT18 *pltB*. Note that all *S. Typhi* strains encode *pltB* on their chromosomes and their DNA sequences are identical. (Adapted from (Lee et al., 2020))

Strain Name	Sequence ID	PltB gene location	Sequence Homology (%)
CT18	Sty1891	1788687-1788274	100
R19_2839	CP046429.1	2684230-2683817	100
2018K-0756	CP044007.1	2313144-2312731	100
WGS1146	CP040575.1	2684661-2684248	100
Ty2 4316STDY6559669	LR590081.1	2568088-2567675	100
311189_217186	CP029646.1	1787549-1787136	100
311189_201186	CP029958.1	1787568-1787155	100
311189_218186	CP029925.1	1788480-1788067	100
343078_273110	CP029846.1	1787719-1787306	100
343078_256191	CP029959.1	1726503-1726090	100
343078_251131	CP029960.1	1788099-1787686	100
343078_228140	CP029962.1	1787808-1787395	100
343078_223175	CP029964.1	1787907-1787494	100
343078_211126	CP029848.1	1787796-1787383	100
343078_203125	CP029850.1	1787691-1787278	100
343078_201101	CP029852.1	1788012-1787599	100
343077_292148	CP029855.1	1787884-1787471	100
343077_286126	CP029856.1	1787067-1786654	100
343077_285138	CP029858.1	1787839-1787426	100
343077_281186	CP029853.1	1726037-1725624	100
343077_278127	CP029863.1	1787499-1787086	100
343077_267164	CP029906.1	1790717-1790304	100
343077_260153	CP029861.1	1787799-1787386	100
343077_255118	CP029907.1	1790401-1789988	100
343077_228157	CP029864.1	1787663-1787250	100
343077_228140	CP029866.1	1827555-1827142	100
343077_215174	CP029868.1	1790707-1790294	100
343077_214162	CP029862.1	1788094-1787681	100
343077_214135	CP029872.1	1787901-1787488	100
343077_213147	CP029897.1	1882683-1882270	100
343077_212159	CP029870.1	1726862-1726449	100
343077_212138	CP029919.1	1790394-1789981	100
343077_211171	CP029873.1	1787670-1787257	100
343076_294172	CP029888.1	1788337-1787924	100
343076_269157	CP029881.1	1827552-1827139	100
343076_253155	CP029890.1	1827830-1827417	100
343076_252143	CP029892.1	1787952-1787539	100
343076_249107	CP029913.1	1787807-1787394	100
343076_248190	CP029882.1	1789926-1789513	100
343076_241106	CP029899.1	1790429-1790016	100

343076_232188	CP029900.1	1787868-1787455	100
343076_227128	CP029875.1	1787865-1787452	100
311189_282186	CP029920.1	1787761-1787348	100
343076_217103	CP029914.1	1790493-1790080	100
343076_202113	CP029915.1	1787839-1787426	100
311189_291186	CP029894.1	1787546-1787133	100
311189_269186	CP029922.1	1787670-1787257	100
311189_268186	CP029883.1	1787273-1786860	100
311189_268103	CP029902.1	1832789-1832376	100
311189_256186	CP029917.1	1787985-1787572	100
311189_255186	CP029885.1	1787948-1787535	100
311189_252186	CP029896.1	1787765-1787352	100
311189_239103	CP029908.1	1789500-1789087	100
311189_232103	CP029918.1	1789005-1788592	100
311189_231186	CP029904.1	1787588-1787175	100
311189_224186	CP029878.1	1787585-1787172	100
311189_223186	CP029880.1	1788850-1788437	100
311189_222186	CP029909.1	1828203-1827790	100
311189_221186	CP029923.1	1787191-1786778	100
311189_220186	CP029886.1	1787992-1787579	100
311189_219186	CP029911.1	1787778-1787365	100
311189_217103	CP029927.1	1789682-1789269	100
311189_216103	CP029928.1	1828252-1827839	100
311189_215186	CP029930.1	1787043-1786630	100
311189_214186	CP029933.1	1787624-1787211	100
311189_213186	CP029936.1	1787792-1787379	100
311189_212186	CP029944.1	1788004-1787591	100
311189_211186	CP029945.1	1790441-1790028	100
311189_210186	CP029946.1	1787772-1787359	100
311189_209186	CP029952.1	1787691-1787278	100
311189_208186	CP029949.1	1787768-1787355	100
311189_208103	CP029932.1	1788052-1787639	100
311189_207186	CP029938.1	1726111-1725698	100
311189_206186	CP029940.1	1789029-1788616	100
311189_205186	CP029950.1	1787384-1786971	100
311189_204186	CP029954.1	1787710-1787297	100
311189_203186	CP029942.1	1787052-1786639	100
311189_202186	CP029956.1	1827716-1827303	100
Ty21a	CP023975.1	2176424-2176837	100
LXYSH	CP030936.1	4243329-4243742	100
OVG_041	LT906560.1	516042-515629	100
SGB90	LT904870.2	2806254-2805841	100
ISP_03_07467_SGB110-sc-1979083	LT905060.2	2662091-2661678	100
1036491	LT906495.1	2657594-2657181	100

ERL024120	LT906494.1	509382-509795	100
1554-sc-2165329	LT906493.1	2657605-2657192	100
E98_3139-sc-1927833	LT905143.1	2366618-2367031	100
H12ESR00755-001A	LT905142.1	369292-368879	100
OVG_041	LT905141.1	1896510-1896923	100
ERL082356	LT905140.1	2441262-2441675	100
2010-007898	LT905139.1	2657610-2657197	100
ty3-243	LT905090.1	4566056-4566469	100
ERL024120	LT905088.1	1520236-1520649	100
1554-sc-2165329	LT905064.1	2657555-2657142	100
lupe_GEN0059-sc-1979081	LT905063.1	2072707-2073120	100
403Ty-sc-1979084	LT905062.1	4644368-4644781	100
ERL12960	LT904894.1	2657509-2657096	100
1016889	LT904893.1	2657582-2657169	100
80-2002	LT904891.1	4585640-4586053	100
H12ESR00394-001A	LT904890.1	2060046-2060459	100
129-0238-M	LT904888.1	4564955-4565368	100
